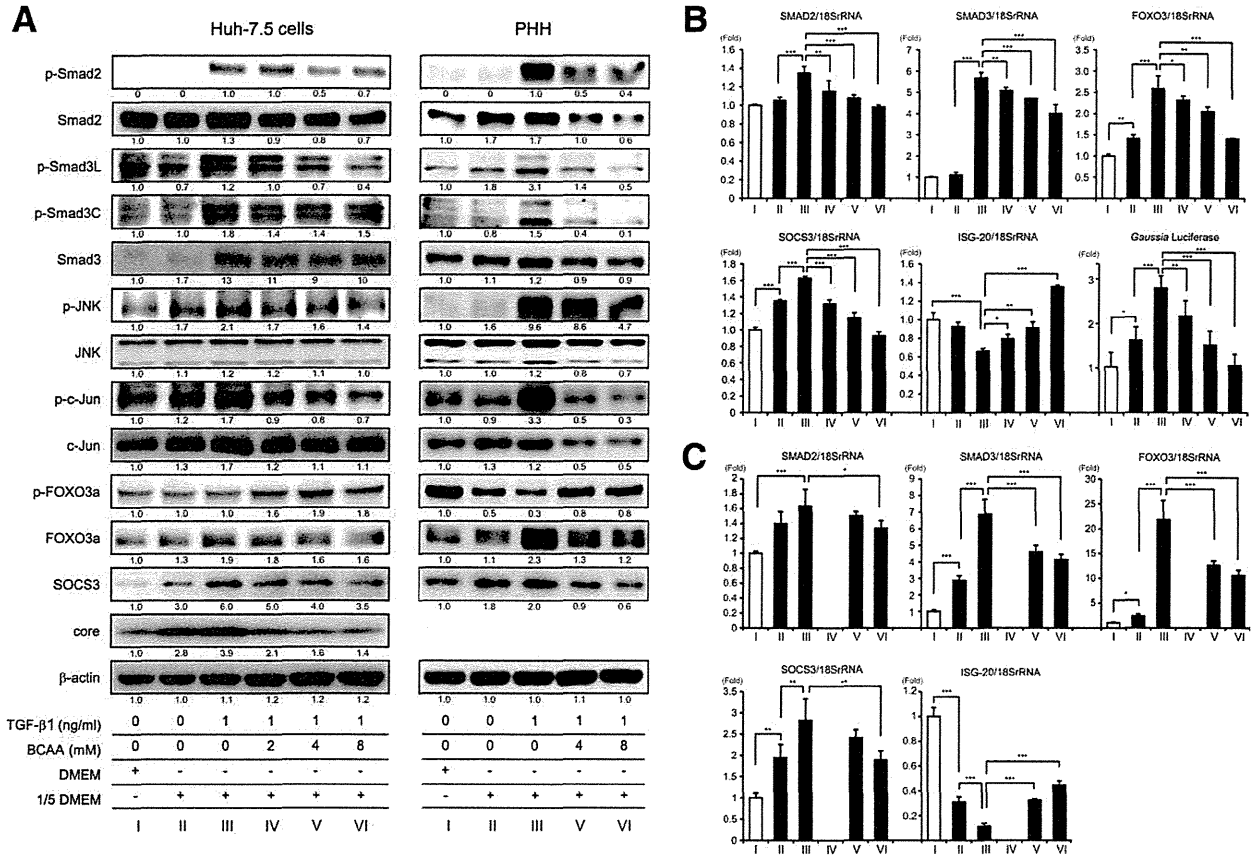

Fig. 7. BCAAs inhibit the effect of malnutrition and TGF-β signaling in Huh-7.5 cells and PHH. A: Western blotting of TGF-β and Foxo3a-Socs3 signaling in Huh-7.5 HCV (+) and PHH treated with amino acid depletion (1/5 DMEM), TGF-β1, and BCAAs. B,C: mRNA expression of TGF-β, Foxo3a-Socs3, and IFN signaling in Huh-7.5 HCV (+) (B) and PHH (C) treated with amino acid depletion (1/5 DMEM), TGF-β1, and BCAA.

blotting analysis showed that BCAAs dose-dependently repressed the expression of p-Smad3L, p-Smad3C, p-JNK, p-c-Jun, Foxo3a, Socs3 (in Huh-7.5 cells and PHH), and HCV core protein (in Huh-7.5 cells), which was induced by amino acid depletion (1/5 DMEM) and TGF-β1 treatment (Fig. 7A). RTD-PCR demonstrated similar mRNA expression patterns (Smad2, Smad3, Foxo3a, and Socs3a) to those obtained by western blotting (Fig. 7B,C), and BCAAs induced the expression of ISG-20 (in Huh-7.5 cells and PHH) and decreased HCV replication in a dose-dependent manner (in Huh-7.5 cells) (Fig. 7B). These results were also confirmed in HCVcc HJ3-5-infected Huh-7 cells (Supporting Fig. 6).

BCAAs and TGF-β RI Potentiate the Anti-HCV Activity of DAAs. Finally, we examined whether BCAAs or TGF-β RI potentiate the anti-HCV activity of DAAs. Amino acid depletion (1/5 DMEM) and TGF-β1 treatment significantly increased HCV replication (deduced from *Gaussia* luciferase activity), and BCAAs (8 mM) and boceprevir (250 nM; NS3 protease inhibitor) inhibited HCV replication to 64% and 50%, respectively (Fig. 8A, black bars). The combination of BCAAs (8 mM) and boceprevir (250 nM) further inhibited HCV replication to 10% and canceled the effect of amino acid depletion (1/5 DMEM) and TGF-β1 treatment, which supported HCV replication (Fig. 8A, compare white and black bars). Similarly, TGF-β RI (10 μM) repressed HCV replication to 60%, and its combination with boceprevir (250 nM) decreased HCV replication to 16% (Fig. 8B, black bars) and canceled the effect of amino acid depletion (1/5 DMEM) and TGF-β1 treatment (Fig. 8A, compare white and black bars). Thus, BCAAs and TGF-β RI had an additive effect on the anti-HCV activity of boceprevir and would be useful for CH-C patients with advanced fibrosis and the IL28B treatment-resistant genotype. A similar effect was obtained by using the NS5A inhibitor BMS-790052; however, its effect was less than that of boceprevir (Supporting Fig. 7).

Discussion

The recently developed DAAs have significantly improved the efficacy of anti-HCV therapy. Triple

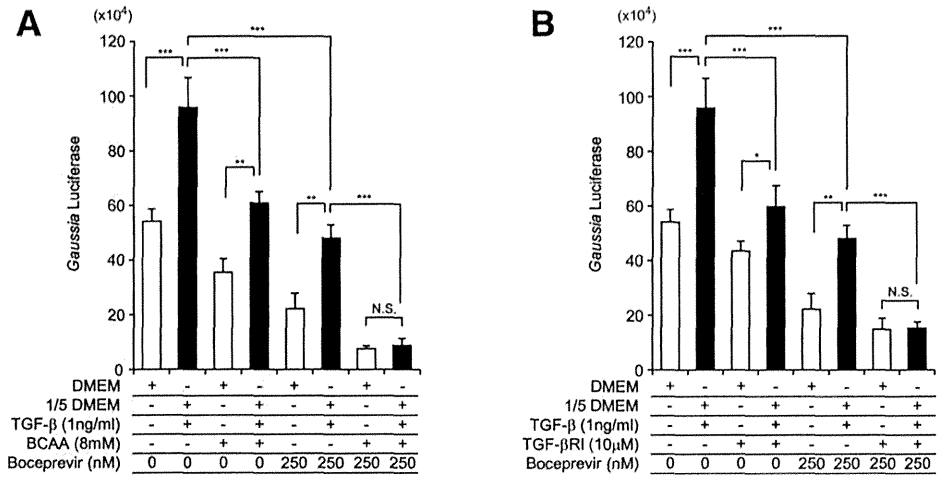

Fig. 8. Anti-HCV activity of boceprevir in combination with BCAAs (A) and TGF-β1 RI (B). HCV replication in Huh-7.5 cells was deduced by *Gaussia* luciferase activity. Boceprevir in combination with BCAAs (A) and TGF-β1 RI (B) efficiently repressed HCV replication in Huh-7.5 cells treated with amino acid depletion (1/5 DMEM) and TGF-β1. The experiments were performed in triplicate and repeated 3 times ($*P < 0.05$, $**P < 0.01$, $***P < 0.001$).

therapy comprising PEG-IFN, RBV, and DAA (e.g., telaprevir or boceprevir) has significantly increased SVR rates; however, its efficacy is poor in difficult-to-cure patients such as those with cirrhosis and the IL28B treatment-resistant genotype.[2,4] An IFN-free regimen using a combination of DAAs would be effective to treat these difficult-to-cure patients; however, the emergence of multiple drug resistant viruses and the high cost of these therapies should be considered carefully in the future. Therefore, standard PEG-IFN plus RBV combination therapy is still useful as an alternative therapy for CH-C.

Previously, we reported that malnutrition in patients with the advanced fibrosis stage of CH-C is associated with IFN resistance and impaired IFN signaling by inhibiting mTORC1 and activating Socs3-mediated IFN inhibitory signaling through the nutrition-sensing transcriptional factor Foxo3a.[6] However, the effect of profibrosis signaling on IFN signaling was not addressed in our previous study. In the present study, using clinical samples and cell lines, we clearly showed that TGF-β signaling inhibits IFN signaling by activating Foxo3a-Socs3-mediated IFN inhibitory signaling (Figs. (1 and 4)) and inhibiting mTORC1 signaling (Fig. 5).

Using Foxo3a promoter-luciferase reporter constructs, we showed that TGF-β1 activated Foxo3a promoter activity through an AP1 transcription factor binding site. Among the components of AP1, c-Jun and probably ATF2, but not c-Fos, were involved in this induction. Previous reports showed that c-Jun and ATF2 were induced by amino acid depletion[13,14] and TGF-β1 treatment,[15,16] although the induction of c-Jun by amino acid depletion was not obvious in PHH in this study. It could be considered that malnutrition and profibrotic signaling cooperatively activated the Foxo3a promoter through the AP1 site and that c-Jun induction was more specifically regulated by TGF-β1 in normal hepatocytes. Mutation of the AP1 binding site (pGL4-FOXO3a [-1340-MT]) abolished the response to amino acid depletion (1/5 DMEM) and TGF-β1 treatment (Fig. 3E; Supporting Fig. 2). Conversely, c-Jun overexpression combined with amino acid depletion (1/5 DMEM) and TGF-β1 treatment activated the Foxo3a promoter by 32-fold (Fig. 3F). In addition, we showed that TGF-β1 inhibited mTORC1 signaling, as demonstrated by the decreased expression of RHEB, p-mTOR, and p-p70S6K (Fig. 5A).

These results were in concordance with gene expression in the liver of CH-C patients. The expression of c-Jun and ATF2 was significantly correlated with Smad2 and Foxo3a expression, respectively (Fig. 4), while the expression of RHEB was significantly negatively correlated with Smad2 expression in the liver of CH-C patients (Fig. 5C). In this study, TGF-β1 and TGF-β2 expression was up-regulated in advanced liver fibrosis, and the expression of TGF-β2 was well correlated with the downstream signaling molecule Smad2 (Fig. 1B-D). Although we could not address the biological differences in TGF-β isoforms in this study, TGF-β1 and TGF-β2 reportedly mediate a similar signaling pathway to induce profibrotic responses.[17] Collectively, TGF-β signaling inhibited IFN signaling by activating Foxo3a-Socs3 IFN inhibitory signaling and

inhibiting mTORC1-IFN stimulating signaling *in vitro* and *in vivo*. Recently, Lee et al. showed that Foxo3a regulates the TGF-β1 promoter directly.[18] Combining their data and ours, there must be positive feedback regulation between TGF-β1 and Foxo3a. Moreover, they identified a polymorphism in Foxo3a (rs12212067: T > G) in which the minor (G) allele was involved in the increased production of TGF-β1 and associated with the inflammatory response.[18] We genotyped the Foxo3a rs12212067 polymorphism in three cell lines and observed TT in Huh-7 and Huh-7.5 and GG in TTNT (Supporting Table 3). Although we could not find a significant difference in Foxo3a promoter activity in response to TGF-β1 among these cell lines (Supporting Fig. 2), further studies should be performed to compare Foxo3a-Socs3 IFN inhibitory signaling among them. Furthermore, it is worthwhile to examine the relationship between the genotype at rs12212067 and treatment response and severity of liver disease in CH-C patients in the future.

Another interesting finding in this study was that TGF-β signaling was related to the IL28B genotype (Fig. 6). The expression of c-Jun was significantly higher in IL28B treatment-resistant minor genotype (TG/GG at rs8099917) patients than in IL28B treatment-sensitive major genotype (TT) patients. Moreover, the expression of c-Jun, Smad2, ATF2, and Socs3 was up-regulated more in IL28B minor genotype patients than in IL28B major genotype patients, especially in those with early stage liver fibrosis (F1-2). The underlying mechanisms of these findings are not known so far; however, we recently reported that the noncanonical WNT signaling ligand WNT5A is up-regulated in the liver of IL28B minor genotype patients and plays a role in treatment resistance.[19] WNT5A reportedly mediates downstream signaling through c-Jun and ATF2 in *Xenopus* cells and human osteosarcoma cells.[20,21] It could be speculated that WNT5A potentiates TGF-β signaling through these transcription factors, although this hypothesis should be tested in the future.

We examined whether BCAAs and TGF-β RI improve the IFN inhibitory signaling induced by malnutrition and TGF-β signaling (Fig. 7). Previously, we demonstrated that BCAAs improved the IFN signaling that was inhibited by malnutrition.[6] In the present study, we found that BCAAs blocked TGF-β signaling by decreasing the levels of p-Smad3L, p-JNK, and c-Jun (Fig. 7A). Consequently, BCAAs decreased the expression of Foxo3a, Socs3, and HCV core protein (Fig. 7). In addition, we found that the combination of BCAAs or TGF-β RI and the NS3 protease inhibitor boceprevir efficiently inhibited HCV replication and canceled the positive effects of malnutrition and TGF-β1 on HCV replication (Fig. 8). A recent report showed that the NS3 protease of HCV mimics TGF-β2 and activates the TGF-β type I receptor.[22] Therefore, the anti-HCV effect of boceprevir could be potentiated in combination with BCAAs or TGF-β RI, which blocked TGF-β signaling and increased IFN signaling. Therefore, the combination of BCAAs or TGF-β RI with DAAs could be useful for the treatment of difficult-to-cure CH-C patients with advanced liver fibrosis and the IL28B treatment-resistant genotype.

In conclusion, we clarified that TGF-β signaling inhibits IFN signaling and is related to the treatment-resistant phenotype of CH-C patients with advanced liver fibrosis and the IL28B treatment-resistant genotype. Furthermore, blocking TGF-β signaling by BCAAs or TGF-β RI could potentiate the anti-HCV effect of DAAs. An oral TGF-β RI small compound, LY2157299, is now being assessed in a phase II trial for the treatment of advanced-stage HCC. Further studies should be performed to address the significance of these compounds for the eradication of HCV in patients with advanced liver fibrosis for preventing HCC.

Acknowledgment: The authors thank Mina Nishiyama for technical assistance.

Author Contributions: Takayoshi Shirasaki performed most experiments and drafted the article; Masao Honda, study design, interpretation of data, and drafting of the article; Tetsuro Shimakami, HCV replication analysis and cellular experiments; Kazuhisa Murai, HCV replication analysis and cellular experiments; Takayuki Shiomoto, HCV replication analysis and cellular experiments; Hikari Okada, HCV replication analysis and cellular experiments; Riuta Takabatake, HCV replication analysis and cellular experiments; Akihiro Tokumaru, HCV replication analysis and cellular experiments; Yoshio Sakai, acquisition of clinical data; Taro Yamashita, acquisition of clinical data; Stanley M. Lemon, study design and interpretation of data; Seishi Murakami, study design and interpretation of data; Shuichi Kaneko, study concept and design.

References

1. Yoshida H, Shiratori Y, Moriyama M, Arakawa Y, Ide T, Sata M, et al. Interferon therapy reduces the risk for hepatocellular carcinoma: national surveillance program of cirrhotic and noncirrhotic patients with chronic hepatitis C in Japan IHIT Study Group. Inhibition of Hepatocarcinogenesis by Interferon Therapy. Ann Intern Med 1999;131:174-181.

2. Trembling PM, Tanwar S, Rosenberg WM, Dusheiko GM. Treatment decisions and contemporary versus pending treatments for hepatitis C. Nat Rev Gastroenterol Hepatol 2013;10:713-728.
3. Hezode C, Fontaine H, Dorival C, Larrey D, Zoulim F, Canva V, et al. Triple therapy in treatment-experienced patients with HCV-cirrhosis in a multicentre cohort of the French Early Access Programme (ANRS CO20-CUPIC) – NCT01514890. J Hepatol 2013;59:434-441.
4. Bruno S, Vierling JM, Esteban R, Nyberg LM, Tanno H, Goodman Z, et al. Efficacy and safety of boceprevir plus peginterferon-ribavirin in patients with HCV G1 infection and advanced fibrosis/cirrhosis. J Hepatol 2013;58:479-487.
5. Tanaka Y, Nishida N, Sugiyama M, Kurosaki M, Matsuura K, Sakamoto N, et al. Genome-wide association of IL28B with response to pegylated interferon-alpha and ribavirin therapy for chronic hepatitis C. Nat Genet 2009;41:1105-1109.
6. Honda M, Takehana K, Sakai A, Tagata Y, Shirasaki T, Nishitani S, et al. Malnutrition impairs interferon signaling through mTOR and FoxO pathways in patients with chronic hepatitis C. Gastroenterology 2011;141:128-140.
7. Okitsu T, Kobayashi N, Jun HS, Shin S, Kim SJ, Han J, et al. Transplantation of reversibly immortalized insulin-secreting human hepatocytes controls diabetes in pancreatectomized pigs. Diabetes 2004;53:105-112.
8. Honda M, Nakamura M, Tateno M, Sakai A, Shimakami T, Shirasaki T, et al. Differential interferon signaling in liver lobule and portal area cells under treatment for chronic hepatitis C. J Hepatol 2010;53:817-826.
9. Yi M, Ma Y, Yates J, Lemon SM. Compensatory mutations in E1, p7, NS2, and NS3 enhance yields of cell culture-infectious intergenotypic chimeric hepatitis C virus. J Virol 2007;81:629-638.
10. Eferl R, Wagner EF. AP-1: a double-edged sword in tumorigenesis. Nat Rev Cancer 2003;3:859-868.
11. Bai X, Ma D, Liu A, Shen X, Wang QJ, Liu Y, et al. Rheb activates mTOR by antagonizing its endogenous inhibitor, FKBP38. Science 2007;318:977-980.
12. Carayol N, Katsoulidis E, Sassano A, Altman JK, Druker BJ, Platanias LC. Suppression of programmed cell death 4 (PDCD4) protein expression by BCR-ABL-regulated engagement of the mTOR/p70 S6 kinase pathway. J Biol Chem 2008;283:8601-8610.
13. Chaveroux C, Jousse C, Cherasse Y, Maurin AC, Parry L, Carraro V, et al. Identification of a novel amino acid response pathway triggering ATF2 phosphorylation in mammals. Mol Cell Biol 2009;29:6515-6526.
14. Fu L, Balasubramanian M, Shan J, Dudenhausen EE, Kilberg MS. Auto-activation of c-JUN gene by amino acid deprivation of hepatocellular carcinoma cells reveals a novel c-JUN-mediated signaling pathway. J Biol Chem 2011;286:36724-36738.
15. Sano Y, Harada J, Tashiro S, Gotoh-Mandeville R, Maekawa T, Ishii S. ATF-2 is a common nuclear target of Smad and TAK1 pathways in transforming growth factor-beta signaling. J Biol Chem 1999;274:8949-8957.
16. Mu Y, Gudey SK, Landstrom M. Non-Smad signaling pathways. Cell Tissue Res 2012;347:11-20.
17. Leask A, Abraham DJ. TGF-beta signaling and the fibrotic response. FASEB J 2004;18:816-827.
18. Lee JC, Espeli M, Anderson CA, Linterman MA, Pocock JM, Williams NJ, et al. Human SNP links differential outcomes in inflammatory and infectious disease to a FOXO3-regulated pathway. Cell 2013;155:57-69.
19. Honda M, Shirasaki T, Shimakami T, Sakai A, Horii R, Arai K, et al. Hepatic interferon-stimulated genes are differentially regulated in the liver of chronic hepatitis C patients with different interleukin 28B genotypes. HEPATOLOGY 2014;59:828-838.
20. Yamanaka H, Moriguchi T, Masuyama N, Kusakabe M, Hanafusa H, Takada R, et al. JNK functions in the non-canonical Wnt pathway to regulate convergent extension movements in vertebrates. EMBO Rep 2002;3:69-75.
21. Yamagata K, Li X, Ikegaki S, Oneyama C, Okada M, Nishita M, et al. Dissection of Wnt5a-Ror2 signaling leading to matrix metalloproteinase (MMP-13) expression. J Biol Chem 2012;287:1588-1599.
22. Sakata K, Hara M, Terada T, Watanabe N, Takaya D, Yaguchi S, et al. HCV NS3 protease enhances liver fibrosis via binding to and activating TGF-beta type I receptor. Sci Rep 2013;3:3243.

Supporting Information

Additional Supporting Information may be found in the online version of this article at the publisher's website.

HEPATOLOGY
Official Journal of the American Association for the Study of Liver Diseases

Gd-EOB-DTPA-Enhanced Magnetic Resonance Imaging and Alpha-Fetoprotein Predict Prognosis of Early-Stage Hepatocellular Carcinoma

Taro Yamashita,[1,2] Azusa Kitao,[3] Osamu Matsui,[3] Takehiro Hayashi,[2] Kouki Nio,[2] Mitsumasa Kondo,[2] Naoki Ohno,[4] Tosiaki Miyati,[4] Hikari Okada,[2] Tatsuya Yamashita,[2] Eishiro Mizukoshi,[2] Masao Honda,[2] Yasuni Nakanuma,[5] Hiroyuki Takamura,[6] Tetsuo Ohta,[6] Yasunari Nakamoto,[7] Masakazu Yamamoto,[8] Tadatoshi Takayama,[9] Shigeki Arii,[10] XinWei Wang,[11] and Shuichi Kaneko[2]

The survival of patients with hepatocellular carcinoma (HCC) is often individually different even after surgery for early-stage tumors. Gadolinium ethoxybenzyl diethylenetriamine pentaacetic acid (Gd-EOB-DTPA)-enhanced magnetic resonance imaging (MRI) has been introduced recently to evaluate hepatic lesions with regard to vascularity and the activity of the organic anion transporter OATP1B3. Here we report that Gd-EOB-DTPA-enhanced MRI (EOB-MRI) in combination with serum alpha-fetoprotein (AFP) status reflects the stem/maturational status of HCC with distinct biology and prognostic information. Gd-EOB-DTPA uptake in the hepatobiliary phase was observed in ~15% of HCCs. This uptake correlated with low serum AFP levels, maintenance of hepatocyte function with the up-regulation of *OATP1B3* and *HNF4A* expression, and good prognosis. By contrast, HCC showing reduced Gd-EOB-DTPA uptake with high serum AFP levels was associated with poor prognosis and the activation of the oncogene *FOXM1*. Knockdown of *HNF4A* in HCC cells showing Gd-EOB-DTPA uptake resulted in the increased expression of *AFP* and *FOXM1* and the loss of *OATP1B3* expression accompanied by morphological changes, enhanced tumorigenesis, and loss of Gd-EOB-DTPA uptake *in vivo*. HCC classification based on EOB-MRI and serum AFP levels predicted overall survival in a single-institution cohort (n = 70), and its prognostic utility was validated independently in a multi-institution cohort of early-stage HCCs (n = 109). *Conclusion*: This noninvasive classification system is molecularly based on the stem/maturation status of HCCs and can be incorporated into current staging practices to improve management algorithms, especially in the early stage of disease. (HEPATOLOGY 2014;60:1674-1685)

Liver cancer is the fifth most commonly diagnosed cancer and the second most frequent cause of cancer death in men worldwide.[1] Among primary liver cancers, hepatocellular carcinoma (HCC) represents the major histological subtype, accounting for 70-86% of cases of primary liver cancer.[1] Several staging systems are currently available for HCC classification and include Tumor Node

Abbreviations: AFP, alpha-fetoprotein; BCLC, Barcelona Clinic Liver Cancer; EOB-MRI, gadolinium ethoxybenzyl diethylenetriamine pentaacetic acid-enhanced magnetic resonance imaging; FOXM1, forkhead box protein M1; Gd-EOB-DTPA, gadolinium ethoxybenzyl diethylenetriamine pentaacetic acid; HCC, hepatocellular carcinoma; HNF4α, hepatocyte nuclear factor 4 alpha; IHC, immunohistochemistry; MRI, magnetic resonance imaging; NOD/SCID, nonobese diabetic, severe combined immunodeficient; OATPs, organic anion transporting polypeptides; qRT-PCR, quantitative reverse-transcription polymerase chain reaction; SI, signal intensity; TNM, tumor node metastasis.

From the [1]Department of General Medicine, Kanazawa University Graduate School of Medical Science, Kanazawa, Ishikawa, Japan; [2]Department of Gastroenterology, Kanazawa University Graduate School of Medical Science, Kanazawa, Ishikawa, Japan; [3]Department of Radiology, Kanazawa University Graduate School of Medical Science, Kanazawa, Ishikawa, Japan; [4]Faculty of Health Sciences, Institute of Medical, Pharmaceutical and Health Sciences, Kanazawa University, Kanazawa, Ishikawa, Japan; [5]Department of Pathology, Kanazawa University Graduate School of Medical Science, Kanazawa, Ishikawa, Japan; [6]Department of Gastroenterologic Surgery, Kanazawa University Graduate School of Medical Science, Kanazawa, Ishikawa, Japan; [7]Second Department of Internal Medicine, Fukui University School of Medicine, Fukui, Japan; [8]Department of Surgery, Institute of Gastroenterology, Tokyo Women's Medical University, Tokyo, Japan; [9]Department of Digestive Surgery, Nihon University School of Medicine, Tokyo, Japan; [10]Department of Hepato-Biliary-Pancreatic Surgery, Tokyo Medical and Dental University, Tokyo, Japan; [11]Laboratory of Human Carcinogenesis, Center for Cancer Research, National Cancer Institute, Bethesda, MD, USA.

Received September 19, 2013; accepted February 20, 2014.

Metastasis (TNM) and Barcelona Clinic Liver Cancer (BCLC) staging, which are based on tumor number and size, vascular invasion, metastatic status, hepatic reserve, and performance status.[2] These systems can provide an approximate estimate of patients' survival, but patients diagnosed at the same disease stage sometimes show a different prognosis. This is most likely because these systems do not include an assessment of the malignant phenotype of the tumor, which would be especially important in those patients diagnosed at the early stage of disease. To overcome these limitations, gene expression profiling technologies have been applied to classify HCC. In particular, the stemness of HCC is currently of great interest because its gene expression profile reflects the malignant nature of the tumor.[3-7] However, the application of these new technologies still needs to be validated externally prior to their implementation in clinical practice.

The hallmark of HCC diagnosis has been image analysis based on vascularity. Gadolinium ethoxybenzyl diethylenetriamine pentaacetic acid (Gd-EOB-DTPA) is a liver-specific magnetic resonance imaging (MRI) contrast agent introduced specifically to improve the detection of liver lesions.[8] Gd-EOB-DTPA-enhanced MRI (EOB-MRI) has been used to evaluate liver tumors in Europe since 2004, in the USA and Japan since 2008, and in China since 2010. Gd-EOB-DTPA is characterized by its rapid and specific uptake by hepatocytes by way of organic anion transporting polypeptides (OATPs) expressed in the sinusoidal membrane. Therefore, Gd-EOB-DTPA uptake in the liver is considered to reflect hepatocyte function.[9] Among OATP1A2, 1B1, 1B3, and 2B1, only OATP1B3 expression was found to correlate with the enhancement ratio on EOB-MRI, indicating that it transports Gd-EOB-DTPA into HCC cells.[10] It is generally accepted that ~85% of HCCs show hypointensity in the hepatobiliary phase of EOB-MRI compared to the noncancerous background liver, with a reduction of OATP1B3 protein or *OATP1B3* gene expression in the tumor.[10,11] However, atypical Gd-EOB-DTPA uptake in the hepatobiliary phase is observed in the remaining 15% of HCCs, and the molecular phenotype and clinical features of these HCCs remain to be elucidated.

We hypothesized that EOB-MRI findings may vary in different tumor subtypes with distinct biology. Therefore, in this study we evaluated the molecular profiles of HCCs in a single-institute cohort determined from the EOB-MRI findings using quantitative reverse-transcription polymerase chain reaction (qRT-PCR), microarray, and immunohistochemistry (IHC) analyses. To clarify the clinical utility of the EOB-MRI findings, we also evaluated the prognosis of a multicenter cohort of patients with early-stage HCC who underwent radical resection.

Materials and Methods

Patients. A total of 417 patients who received surgical resection for HCC were enrolled in this study. Seventy patients underwent EOB-MRI for the diagnosis of HCC and received surgical resection at Kanazawa University Hospital from 2008 to 2011. Survival analysis was performed in this single-institute cohort (Cohort 1) and prognosis was evaluated every 6 months. The final evaluation of survival was performed in October 2011. From these 70 patients, 62 tumor and nontumor samples were snap-frozen in liquid nitrogen and used for qRT-PCR.

For microarray analysis, we assessed 238 patients who received surgical resection of HCC at the Liver Cancer Institute of Fudan University. EOB-MRI was not performed in these patients because Gd-EOB-DTPA had not yet been introduced in China. Their clinicopathologic characteristics and prognostic data have been described previously.[12]

To evaluate the survival of early-stage HCCs, we enrolled 109 patients who received EOB-MRI and surgical resection at Tokyo Medical and Dental University Hospital, Tokyo Women's Medical University Hospital, Nihon University School of Medicine Itabashi Hospital, Niigata University Medical & Dental Hospital, Hyogo College of Medicine Hospital, or Kurume

Supported by Health and Labor Sciences Research Grants for "Development of novel molecular markers and imaging modalities for earlier diagnosis of hepatocellular carcinoma," Grants from the Ministry of Education, Culture, Sports, Science, and Technology of Japan, the National Cancer Center Research and Development Fund (23-B-5), and the Intramural Research Program Grant (Z01 BC 010313) of the Center for Cancer Research, US National Cancer Institute.

Address reprint requests to: Taro Yamashita, M.D., Ph.D., Assistant Professor, Department of Gastroenterology/General Medicine, Kanazawa University Graduate School of Medical Science, 13-1 Takara-Machi, Kanazawa, Ishikawa 920-8641, Japan. E-mail: taroy@m-kanazawa.jp; fax: +81-76-234-4250.

View this article online at wileyonlinelibrary.com.

DOI 10.1002/hep.27093

Potential conflict of interest: Dr. Matsui is on the speakers' bureau for Bayer.

University Hospital from 2008 to 2009 (Cohort 2). The prognosis of these patients was evaluated every year, and the final evaluation of survival was performed in February 2012.

This study was approved by the Institutional Review Board at each study center and all patients provided written informed consent.

EOB-MRI. EOB-MRI was performed before surgical resection using a 1.5 or 3.0 Tesla MRI system with a fat-suppressed 2D or 3D gradient echo T1-weighted sequence (relaxation time / echo time [TR/TE] = 3.2-3.6/1.6-2.3 ms, flip angle 10-15°, field of view 33-42 cm, matrix 128-192 × 256-512, slice thickness 4.0-8.0 mm). A dose of 0.025 mmol/kg Gd-EOB-DTPA (Primovist; Bayer Schering Pharma, Berlin, Germany) was injected intravenously and the hepatobiliary phase was obtained at 15-20 minutes after the injection.

All abdominal MRI data of the HCC patients were generated at Kanazawa University Hospital and image analysis was performed retrospectively by two radiologists (A.K. and O.M.) without knowledge of the clinical and pathological results. The signal intensity (SI) of the tumor was measured within the region of interest, which was determined as the maximum oval area at the largest section of the tumor. The SI of the adjacent background liver was also measured within a region of interest of the same size, while avoiding large vessels. The nodules were classified into the two following types: hypointense HCC, which was defined as showing a lower SI than that of the surrounding liver (tumor SI / background SI <1.0) in the hepatobiliary phase, and hyperintense HCC, which was defined as showing an equal or higher SI (tumor SI / background SI ≥ 1.0).

For the mouse study, EOB-MRI was performed using a 0.4 T MRI system with a fat-suppressed 3D gradient echo T1-weighted sequence (TR/TE = 66.5/4.0 ms, flip angle 40°, field of view 10 cm, matrix 224 × 192, slice thickness 1.0 mm). A dose of 0.025 mmol/kg Gd-EOB-DTPA (Bayer Schering Pharma) was injected through the tail vein, and the hepatobiliary phase was obtained at 12-20 minutes after the injection.

Xenotransplantation of Primary HCC in Immunodeficient Mice and* HNF4A *Knockdown. Primary HCC tissue was dissected and digested in 1 mg/mL type 4 collagenase solution (Sigma-Aldrich Japan, Tokyo, Japan) at 37°C for 15-30 minutes. Contaminated red blood cells were lysed with an ammonium chloride solution (STEMCELL Technologies, Vancouver, BC, Canada) on ice for 5 minutes. $CD45^+$ leukocytes and annexin V^+ apoptotic cells were removed by an autoMACS-pro cell separator and magnetic beads (Miltenyi Biotec, Tokyo, Japan). The cells were suspended 1:1 in 200 μL Dulbecco's modified Eagle's medium (DMEM) and Matrigel (BD Biosciences) and injected subcutaneously into 6-week-old NOD/SCID mice (NOD/NCrCRl-*Prkdc*^{scid}) purchased from Charles River Laboratories (Wilmington, MA). EOB-MRI was performed to evaluate Gd-EOB-DTPA uptake in the subcutaneous tumor at the hepatobiliary phase, and the subcutaneous tumor was dissected and digested as described above, and subsequently cultured in DMEM. *HNF4A* knockdown was performed using pGFP-V-RS vectors (OriGene Technologies, Rockville, MD), allowing stable delivery of the short hairpin RNA (shRNA) expression cassette against *HNF4A* or scramble sequence into host cells by way of a replication-deficient retrovirus. Infected HCC cells were grown in DMEM containing 1 μg/mL puromycin (Sigma-Aldrich Japan) for 7 days to establish stable shRNA-expressing HCC cells. Western blotting and immunofluorescence analyses were performed using an antihuman HNF4α C11F12 antibody (Cell Signaling Technology, Danvers, MA) and a mouse monoclonal antihuman OATP1B3 MDQ/5F260 antibody (Novus Biologicals, Littleton, CO), essentially as described previously.[13] Control or Sh-HNF4A-transfected HCC cells were injected subcutaneously into NOD/SCID mice, and tumor volume and survival were evaluated every 2-3 days. The protocol was approved by the Kanazawa University Animal Care and Use Committee and the Kanazawa University Genetic Modification Experiment Committee.

Microarray Analysis. The 238 HCC cases from the Liver Cancer Institute of Fudan University with available microarray data and clinicopathologic and prognostic data have been described previously.[12] BRB-ArrayTools software (v. 3.8.1) was used for class comparison analysis. Hierarchical clustering analysis was performed with Genesis software (v. 1.6.0 beta). Canonical pathway and transcription factor analyses were performed using MetaCore software (http://www.genego.com). Interaction network analysis was performed using Ingenuity Pathway Analysis software (http://www.ingenuity.com).

qRT-PCR Analysis. Total RNA was extracted using an RNeasy Mini Kit (Qiagen, Valencia, CA) according to the manufacturer's instructions. The expression of selected genes was determined in triplicate using the Applied Biosystems 7900HT Sequence Detection System (Applied Biosystems, Foster City, CA) and the $-\Delta\Delta CT$ method. The following probes were used: *AFP*, Hs00173490_m1; *FOXM1*, Hs01073586_m1; *OATP1B3*, Hs00251986_m1; *CYP3A4*, Hs00430021_m1; and *18S*, Hs99999901_s1 (Applied Biosystems).

IHC Analysis. IHC was performed using Envision+ kits (Dako Japan, Tokyo, Japan) as described previously.[14] Mouse monoclonal antihuman Ki-67 antigen MIB-1 (Dako Japan), mouse monoclonal antihuman OATP1B3 MDQ/5F260 (Novus Biologicals), rabbit monoclonal antihuman HNF4α C11F12 (Cell Signaling Technology), mouse monoclonal antihuman FOXM1 0.T.181 (Abcam, Cambridge, MA), mouse monoclonal antihuman glypican-3 1G12 (BioMosaics, Burlington, VT), and mouse monoclonal antiglutamine synthetase clone GS-6 (Millipore, Billerica, MA) antibodies were used. The staining area and intensities were evaluated in each sample and graded from 0-3 (0, 0-5%; 1, 5-25%; 2, 25-50%; 3, >50%) and 0-2 (0, negative; 1, weak; 2, strong), respectively. The sum of the area and intensity scores of each marker (IHC score) were calculated. Samples were defined as marker-high (IHC score ≥3) or -low (IHC score ≤2). The Ki-67 labeling index was calculated as described previously.[14]

Statistical Analysis. Mann-Whitney, χ^2, Fisher's exact, and Kruskal-Wallis tests were used to compare the clinicopathologic characteristics and gene expression data. The correlation of the gene expression data was evaluated by Spearman's rank correlation coefficient. Kaplan-Meier survival analysis with the log-rank test was performed to compare patient survival. All analyses were performed using GraphPad Prism software v. 5.0.1 (GraphPad Software, San Diego, CA).

Results

EOB-MRI Findings and Molecular Characteristics of HCC. Nine of the 70 HCC cases (12.9%) in Cohort 1 were diagnosed with hyperintense HCC on EOB-MRI (Fig. 1A). Analysis of the clinicopathologic characteristics of hyper- or hypointense HCCs revealed that hyperintense HCCs were significantly associated with low serum alpha-fetoprotein (AFP) levels (Table 1). There was no significant difference between hyper- and hypointense HCCs in terms of other factors, including tumor size, number, TNM and BCLC stages, surgical procedures, and elapsed time between MRI and surgery. We confirmed the overexpression of OATP1B3, a transporter responsible for the uptake of Gd-EOB-DTPA in hepatocytes, in hyperintense HCCs by qRT-PCR and IHC (Fig. 1B).

To understand the transcriptomic characteristics of HCCs overexpressing *OATP1B3*, we analyzed the microarray data of an additional 238 HCC cases.[12] *OATP1B3*-high and -low HCCs were defined as HCCs with a T/N ratio ≥1.0 and <1.0, respectively, as used for the evaluation of hyperintense HCCs (tumor SI / background SI ≥1.0). The frequency of *OATP1B3*-high HCCs was 15.1% (36 of the 238 HCC cases), almost comparable to the frequency of hyperintense HCCs reported thus far. Class-comparison analysis yielded a total of 974 genes that were differentially expressed between *OATP1B3*-high and -low HCCs ($P < 0.001$). Hierarchical cluster analysis of this 974 gene set (*OATP1B3* gene signature) separated HCCs into two branches (B1 and B2) (Fig. 1C). Thirty-four of the 36 *OATP1B3*-high HCCs (blue box) were classified in the left branch (B1), while *OATP1B3*-low HCCs were clustered in both branches. The prognosis of HCC patients clustered in B1 was significantly better than those clustered in B2 ($P = 0.02$) (Supporting Fig. S1). Genes associated with mature hepatocyte function such as *ALB* and *CYP3A4* were significantly up-regulated in the HCCs clustered in B1, and the known hepatic stem/progenitor markers *KRT19* and *EPCAM*, as well as the G1/S cell cycle marker *MKI67*, were significantly up-regulated in the HCCs clustered in B2 (Fig. 1D).

Pathway analysis indicated that *OATP1B3*-high HCCs showed maintenance of mature hepatocyte function and decreased cell proliferation and Wnt signaling (Fig. 1E), which are known to be activated during liver development and regeneration.[15] Transcription factor analysis identified eight genes (*HNF4A, NFIA, NR3C1, NR1I3, ESR1, NR1H3, MLXIPL*, and *NFE2L2*) as candidate transcription factors that were significantly activated in *OATP1B3*-high HCCs ($P < 0.005$) (Fig. 1F). These transcription factors are known to play a pivotal role in liver development and in the regulation of hepatocyte functions including lipid, bile, carbohydrate, and xenobiotic metabolism.[16] By contrast, only one gene (*FOXM1*) was identified as a candidate transcription factor activated in *OATP1B3*-low HCCs. The forkhead box M1 (FOXM1) transcription factor is known to be activated during liver regeneration and regulation of the cell cycle.[17] We investigated the expression of the two transcription factors most strongly activated (*HNF4A* encoding hepatocyte nuclear factor 4 alpha [HNF4α]) or inactivated (*FOXM1*) in hyperintense HCCs (Fig. S2) and validated the results using microarray analyses (Fig. 2A,B).

Although the microarray data revealed distinct molecular portraits associated with liver development and the maturation programs present in hyper- and hypointense HCCs, hierarchical cluster analysis further indicated that a subset of hypointense HCCs (corresponding to the *OATP1B3*-low HCCs clustered in B1)

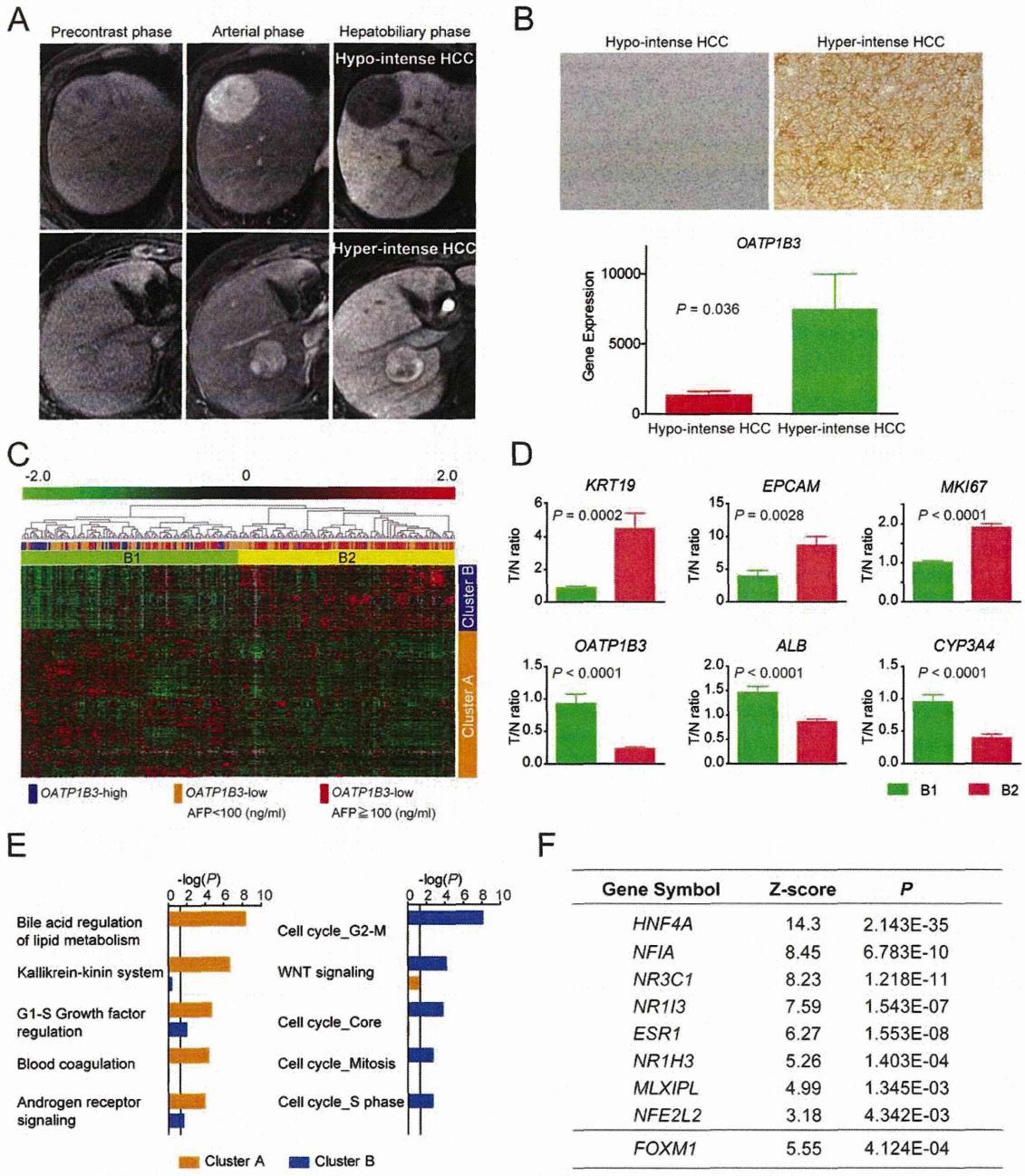

F

Gene Symbol	Z-score	P
HNF4A	14.3	2.143E-35
NFIA	8.45	6.783E-10
NR3C1	8.23	1.218E-11
NR1I3	7.59	1.543E-07
ESR1	6.27	1.553E-08
NR1H3	5.26	1.403E-04
MLXIPL	4.99	1.345E-03
NFE2L2	3.18	4.342E-03
FOXM1	5.55	4.124E-04

Fig. 1. Molecular profiles of HCCs corresponding to the EOB-MRI findings. (A) Representative MRI scans of hypo- and hyperintense HCCs in the precontrast, arterial, and hepatobiliary phases. The T/N signal intensity ratios of the images in the hepatobiliary phase were 0.47 (upper panel) and 1.07 (lower panel). (B) Upper panel: Representative photomicrographs of IHC staining with an anti-OATP1B3 antibody in hypo- and hyperintense HCCs. Lower panel: *OATP1B3* expression in hypo- and hyperintense HCCs. (C) The expression patterns of *OATP1B3* signatures in *OATP1B3*-high (blue box), *OATP1B3*-low AFP-low (<100 ng/mL) (orange box), and *OATP1B3*-low AFP-high (≥100 ng/mL; red box) after hierarchical clustering of genes and samples, shown as a heat map image. Red indicates a high expression level; green indicates a low expression level. *OATP1B3*-high HCCs and *OATP1B3*-low AFP-high HCCs were clustered in B1 (green bar) and B2 (yellow bar), respectively. (D) Representative expression of genes in clusters A (*KRT19, EPCAM*, and *MKI67*) and B (*OATP1B3, ALB*, and *CYP3A4*). The green and orange bars indicate HCCs clustered in B1 and B2, respectively. (E) The activated pathways are identified in clusters A (orange bar) and B (blue bar). (F) Genes encoding transcription factors activated or inactivated in *OATP1B3*-high HCCs.

might show similar gene expression profiles to those observed in hyperintense HCCs. Since serum AFP levels are reportedly related to the stem/maturation subtypes of HCCs with different gene expression profiles,[12] we analyzed the characteristics of *OATP1B3*-low HCCs in 238 cases according to serum AFP levels. Interestingly, *OATP1B3*-low HCCs assigned to the left branch (B1) had low serum AFP

Table 1. Characteristics of HCCs Classified by EOB-MRI in Cohorts 1 and 2

Characteristics	Cohort 1			Cohort 2		
	Hyperintense (n = 9)	Hypointense (n = 61)	P*	Hyperintense (n = 9)	Hypointense (n = 100)	P*
Age (years, mean ± SE)	66.2 ± 3.6	64.6 ± 1.2	0.21	67.2 ± 2.0	66.2 ± 1.0	1.0
Sex (male/female)	7/2	44/17	0.72	9/0	79/21	0.13
Etiology (HBV/HCV/other)	2/3/4	14/23/24	0.95	1/6/0/2	22/56/2/20	0.52
Liver cirrhosis (yes/no)	5/4	33/28	0.94	2/7	42/58	0.25
AFP (ng/mL, mean ± SE)	12.4 ± 1.9	2,157 ± 866	0.03	7.0 ± 2.2	188.4 ± 74	0.03
Histologic grade†						
I-II	1	12		2	16	
II-III	8	38		7	74	
III-IV	0	11	0.25	0	10	0.57
Tumor size (cm, mean ± SE)	4.0 ± 0.9	4.4 ± 0.4	0.79	3.3 ± 0.4	2.6 ± 0.1	0.09
Tumor number (single/multiple)	7/2	48/13	0.95	8/1	86/14	0.81
Macroscopic portal vein invasion (yes/no)	1/8	5/56	0.58	0/9	0/100	
Microscopic portal vein invasion (yes/no)	2/7	27/34	0.21	0/9	11/89	0.59
Tumor-node-metastasis classification (I/II/III)	6/2/1	29/28/4	0.40	7/2/0	75/25/0	0.85
BCLC stage (0/A/B/C)	0/7/1/1	4/30/22/5	0.34	0/9/0/0	27/73/0/0	0.07
Elapsed time between MRI and surgery (days, mean ± SE)	47.0 ± 8.4	51.5 ± 3.2	0.73	17.3 ± 5.0	20.6 ± 3.0	0.50
Surgical procedure (partial resection or segmentectomy/ lobectomy or extended lobectomy)	6/3	35/26	0.60	8/1	86/14	1.0

*Mann-Whitney test, Fisher's exact test, or χ^2 test.
†Edmondson-Steiner.

levels (<100 ng/mL: orange box, Fig. 1C), while the majority of AFP-high (≥100 ng/mL) HCCs (red box, Fig. 1C) were clustered in the right branch (B2). Consistently, the *OATP1B3* gene signature significantly predicted the serum AFP status of 238 HCCs ($P < 0.05$) (Tables S1-3).

OATP1B3 and AFP Expression in HCC Subtypes Related to Stem/Maturational Status. Molecular profiling of tissue samples may be useful for predicting the survival of HCC patients, as reported previously.[18,19] However, such an approach should be established before being applied routinely in a clinical setting. The above data prompted us to hypothesize that EOB-MRI findings and serum AFP levels, in place of molecular profiling techniques, have the potential to categorize HCCs (EOB-AFP classification), thus serving as predictors of survival. We categorized HCCs into three groups (class A: hyperintense HCC, class B: hypointense and AFP-low [<100 ng/mL] HCC, and class C: hypointense and AFP-high [≥100 ng/mL] HCC). The clinicopathologic characteristics of patients with class A, B, and C HCCs in Cohort 1 are shown in Table S4.

We investigated the expression of HNF4α and FOXM1 as well as the G1/S marker Ki-67 by IHC according to the EOB-AFP classification system in Cohort 1 (Fig. 2C). HNF4α was most abundantly expressed in class A HCCs, but its expression was decreased in class B and C HCCs. By contrast, the expression of FOXM1 and Ki-67 was highest in class C HCCs, significantly decreased in class B HCCs, and not detected in class A HCCs. The mean Ki-67 labeling indices in class A, B, and C HCCs were 2.8%, 9.4%, and 18.2%, respectively ($P < 0.0001$) (Fig. 2D). The differences in FOXM1 and HNF4α expression among class A, B, and C HCCs were statistically significant (Fig. 2E).

We further investigated the expression of five markers (glypican 3, GPC-3; lymphatic vessel endothelial hyaluronan receptor 1, LYVE-1; survivin; heat shock 70 kDa protein, HSP70; and glutamine synthetase, GS), known to be differentially expressed between dysplastic nodule and well-differentiated HCC,[20,21] to clarify if the molecular alterations in early-stage hepatocarcinogenesis can be detected differentially in EOB-AFP class A, B, and C HCCs. IHC analysis suggested no differential expression of LYVE-1, survivin, and HSP70 among the EOB-AFP classes (data not shown). Interestingly, GS was most abundantly expressed in class A HCCs, and its expression was relatively decreased in class B and C HCCs with borderline significance ($P = 0.06$) (Fig. S3A,B). In contrast, GPC-3 expression was highest in class C HCCs and relatively decreased in class A and B HCCs with statistical significance ($P = 0.03$). We investigated the microarray data of 238 independent HCC cases and validated the positive correlation between *OATP1B3* and *GLUL* (encoding GS) and the weak negative correlation between *OATP1B3* and *GPC3* (encoding GPC-3).

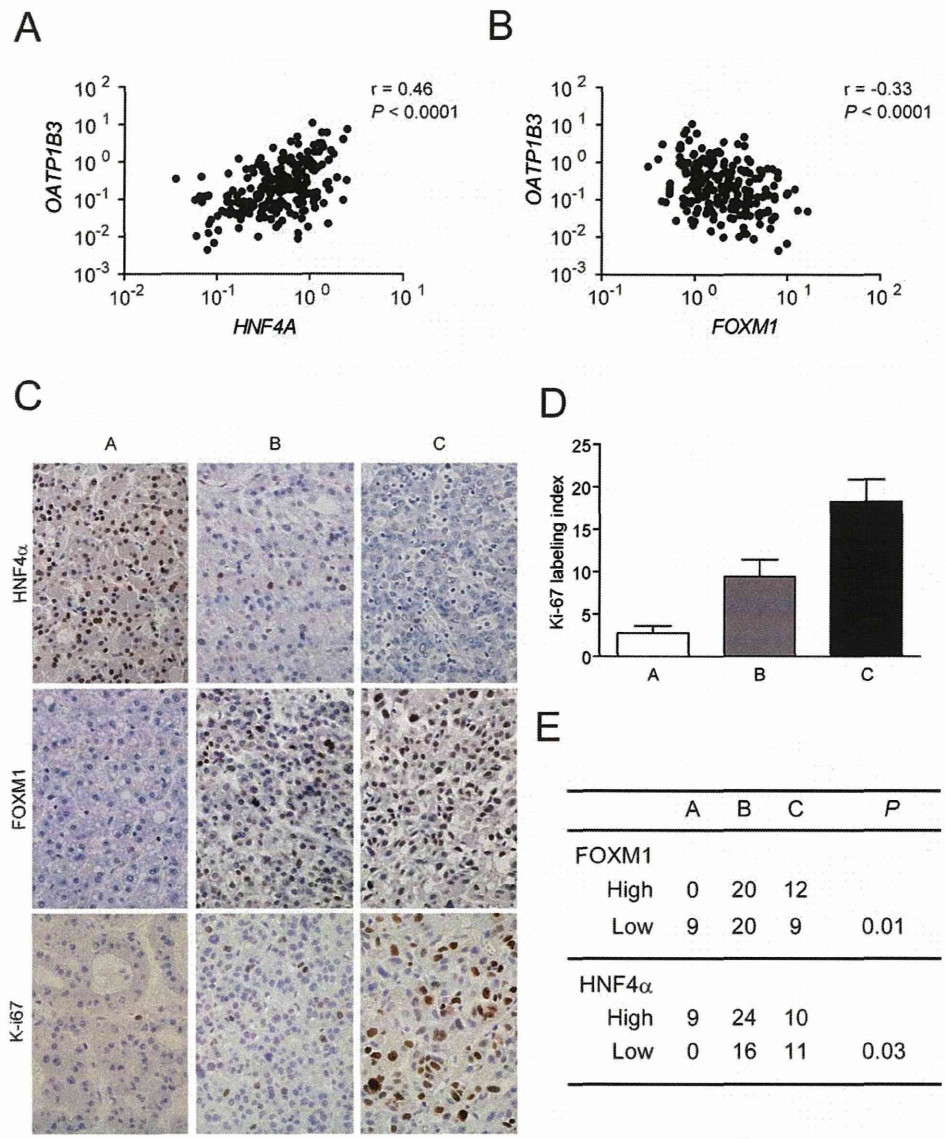

E

	A	B	C	P
FOXM1				
High	0	20	12	
Low	9	20	9	0.01
HNF4α				
High	9	24	10	
Low	0	16	11	0.03

Fig. 2. Transcriptional programs of HCCs corresponding to the EOB-MRI findings and serum AFP. (A,B) Scatterplot analyses of the microarray data of 238 HCCs. (C) Representative photomicrographs of IHC staining with anti-HNF4α, anti-FOXM1, and anti-Ki-67 antibodies in class A, B, and C HCCs, according to the EOB-AFP classification. (D) Ki-67 labeling index in class A, B, and C HCCs. (E) Summary of FOXM1 and HNF4α expression in class A, B, and C HCCs.

Regulation of Gd-EOB-DTPA Uptake and Tumorigenic Capacity by HNF4α in Hyperintense HCC. Microarray and IHC analyses suggested the activation of transcription factor HNF4α in hyperintense HCC, but its role in the maintenance of hepatocyte function and Gd-EOB-DTPA uptake has not yet been clarified. To directly explore the role of HNF4α in Gd-EOB-DTPA uptake and tumorigenic capacities, we transplanted tumor cells from hyper- and hypointense primary HCC specimens into NOD/SCID mice (Fig. 3A). We confirmed on EOB-MRI that Gd-EOB-DTPA uptake capacity was relatively maintained in the secondary xenotransplanted tumors that developed in the subcutaneous lesions of the mice (Fig. 3B).

Using a retrovirus system *in vitro*, we then introduced shRNA targeting *HNF4A* (Sh-HNF4A) or scramble (Sh-Scr) into tumor cells obtained from a hyperintense HCC. We confirmed the reduction of HNF4α protein expression in Sh-HNF4A-transfected cells compared with Sh-Scr-transfected cells by western blotting (Fig. 3C, left panel). Interestingly, *HNF4A* knockdown resulted in a modest increase in *AFP* and *FOXM1* expression and a dramatic decrease in *CYP3A4* and *OATP1B3* expression (Fig. 3C, right panel). It also resulted in the loss of OATP1B3 protein expression, and striking morphological changes were confirmed by immunofluorescence and phase-contrast microscopy (Fig. 3D). Sh-HNF4A-transfected cells displayed long, thin cell shapes with neurite-like extensions, whereas Sh-Scr-transfected cells were relatively smooth and round. Sh-Scr- or Sh-HNF4A-transfected cells were further injected subcutaneously into NOD/SCID mice, and aggressive tumor growth accompanied with the loss of Gd-EOB-DTPA uptake capacity was

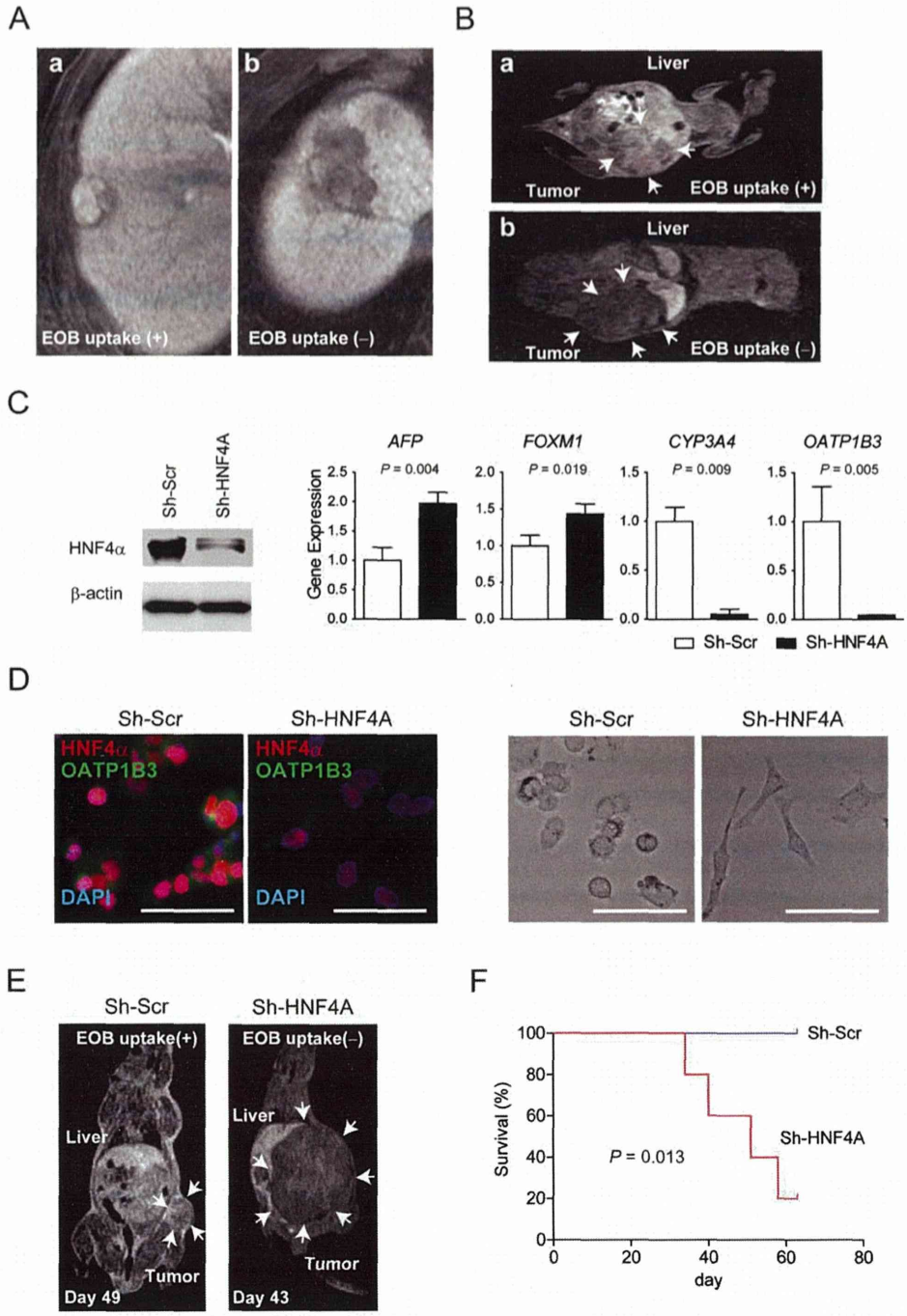

Fig. 3. HNF4α regulates a mature hepatocyte-like, less aggressive HCC phenotype coupled with Gd-EOB-DTPA uptake in hyperintense HCC. (A) MRI scans of hyperintense (a) and hypointense (b) HCCs in the hepatobiliary phase before surgery. The T/N signal intensity ratios of the images in the hepatobiliary phase were 1.02 (left panel) and 0.49 (right panel). Surgically resected specimens were subsequently used for mouse xenotransplantation. (B) MRI scans of NOD/SCID mouse xenotransplanted with hyperintense (a) and hypointense (b) HCCs in the hepatobiliary phase. The T/N signal intensity ratios of the images were 0.82 (upper panel) and 0.45 (lower panel). (C) Left panel: Expression of HNF4α protein by western blotting. Hyperintense HCC cells were harvested in dishes and treated with retroviruses encoding an expression cassette against *HNF4A* (Sh-HNF4A) or scramble sequence (Sh-Scr). Right panel: qRT-PCR of *AFP, FOXM1, CYP3A4*, and *OATP1B3* in hyperintense HCC cells transfected with Sh-Scr or Sh-HNF4A. (D) Left panel: Immunofluorescence analysis of HNF4α (red) and OATP1B3 (green) in hyperintense HCC cells transfected with Sh-Scr or Sh-HNF4A (scale bar = 100 μm). Right panel: Representative photomicrographs of hyperintense HCC cells transfected with Sh-Scr or Sh-HNF4A (scale bar = 100 μm). (E) MRI scans of NOD/SCID mouse xenotransplanted with hyperintense HCC cells transfected with Sh-Scr (day 49 after transplantation) or Sh-HNF4A (day 43 after transplantation). The T/N signal intensity ratios of the images in the hepatobiliary phase were 0.65 (left panel) and 0.34 (right panel). (F) Survival of NOD/SCID mice xenotransplanted with hyperintense HCC cells transfected with Sh-Scr (n = 5) or Sh-HNF4A (n = 5).

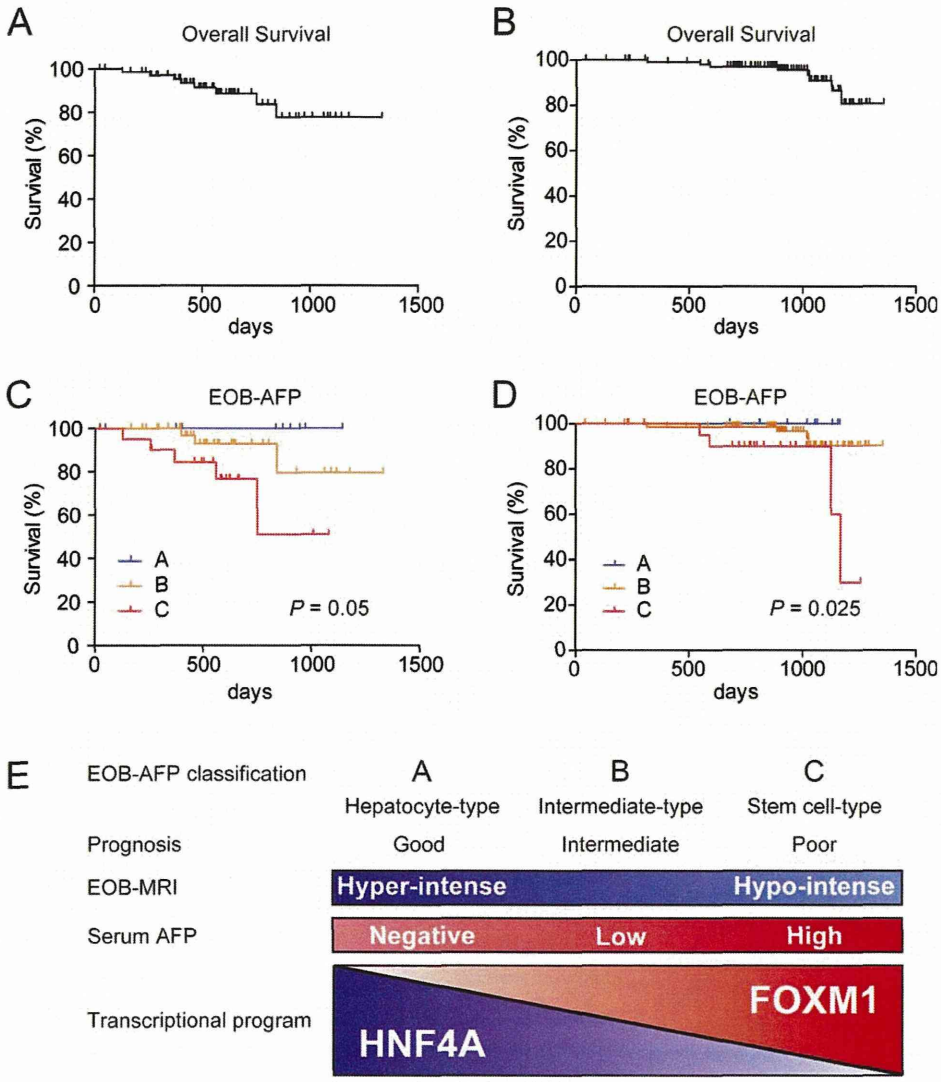

Fig. 4. Prognostic utility of the EOB-AFP classification. (A,B) Overall survival curves of Cohorts 1 (A) and 2 (B). (C,D) Overall survival curves of Cohorts 1 (C) and 2 (D) according to the EOB-AFP classification. (E) The EOB-AFP classification system and its molecular basis.

observed in Sh-HNF4A-transfected cells, whereas Sh-Scr-transfected cells still showed Gd-EOB-DTPA uptake with less tumorigenic capacity (Fig. 3E). Mice xenotransplanted with Sh-HNF4A-transfected cells had a worse prognosis compared with those xenotransplanted with Sh-Scr-transfected cells (Fig. 3F), indicating a crucial role for HNF4α in the maintenance of a mature hepatocyte-like, less aggressive HCC phenotype coupled with Gd-EOB-DTPA uptake capacity.

Prognosis of Early-Stage HCC by EOB-AFP Classification. Finally, we evaluated the prognosis of patients with HCC diagnosed by EOB-MRI and serum AFP. To exclude the potential effect of lead-time bias on survival analysis for HCCs at different stages, we evaluated the power of the EOB-AFP classification system to predict the prognosis of patients with early-stage BCLC stage 0 or A HCCs diagnosed by EOB-MRI in an independent multicenter cohort (Cohort 2). Nine of the 109 HCC cases (8.3%) were diagnosed with hyperintense HCCs and were found to be significantly associated with low serum AFP levels (Table 1). The clinicopathologic characteristics of the patients defined by the EOB-AFP classification are shown in Supporting Table 5. The median follow-up times in Cohorts 1 and 2 were 569 and 932 days, respectively. The 3-year overall survival rates in Cohorts 1 and 2 were 77.7% and 90.9%, respectively (Fig. 4A,B). The prognosis of HCC patients was not separated by TNM or BCLC stages because most of these patients were diagnosed at early stages (Fig. S4A-D); nevertheless, the EOB-AFP classification system robustly stratified HCCs according to survival with statistically significant differences between the classes (Fig. 4C,D). EOB-AFP class A patients had 100% overall survival, whereas class C patients had 30% overall survival at 1,200 days after radical resection in Cohort 2.

The prognosis of HCC patients stratified by the EOB-AFP classification was most likely affected by the malignant nature of the tumor at surgical resection, because EOB-AFP class C patients showed a 40-60% recurrence-free survival rate, whereas class A patients had a 88-100% recurrence-free survival rate at 1 year after radical resection in both cohorts (Fig. S5).

Altogether, our data, for the first time, revealed that the prognosis of early-stage HCC patients is heterogeneous and related to the malignant phenotypes of the tumors, even after successful treatment by radical resection. The EOB-AFP classification system reflects the malignant nature of the tumor and predicts the survival of early-stage HCC patients prior to surgery.

Discussion

Among several HCC staging systems currently used,[2] the BCLC system is recommended because it is linked to treatment strategy.[22] The assessment of the malignant nature of tumors coupled with current staging systems will supplement the management of early-stage HCC[23] because early recurrence after potentially curative treatment may be associated with the characteristics of the resected tumor rather than the development of a *de novo* HCC in the background liver.[24] Molecular profiling approaches have tried to evaluate the malignant features of HCCs and the surrounding noncancerous liver tissue,[3-6,12,18] although the evaluation of the potential clinical application of these approaches is ongoing. Our EOB-AFP classification system is molecularly related to the *OATP1B3* gene signature, which can be used to classify HCCs according to their stem/maturational status. Interestingly, the differential expression of *OATP1B3* was also noted in two HCC subtypes associated with the stem/maturational status, as reported recently by our group (hepatic stem cell-like and mature hepatocyte-like HCC)[12] and others (hepatoblast-type and hepatocyte type)[4] (Fig. S6). As expected, all class A HCCs were categorized as mature hepatocyte-like HCC in Cohort 1 (data not shown). The stem/maturational status defined by the EOB-AFP classification is most likely regulated by at least two transcription factors: HNF4α and FOXM1 (Fig. 4E).

HNF4α was first discovered as a liver-enriched nuclear orphan receptor activating the transcription of transthyretin genes, and it is known to regulate bile acid and cholesterol metabolism.[25] The liver-specific loss of *HNF4A* in adult mice results in hepatocyte proliferation,[26] whereas the introduction of *HNF4A* suppresses HCC growth.[27,28] Furthermore, a recent study suggested a role for *HNF4A* as a tumor suppressor in inflammation-related hepatocarcinogenesis through the regulation of microRNAs.[29] The present study demonstrated a crucial role for HNF4α in maintaining a hepatocyte-like, less aggressive phenotype coupled with Gd-EOB-DTPA uptake in a class A HCC by directly modifying *HNF4A* gene expression. Thus, *HNF4A* may work as a tumor suppressor gene and inhibit the progression of HCC, which may be related to the good prognosis of class A HCCs.

FOXM1 belongs to the forkhead superfamily of transcription factors and regulates a myriad of biologic processes including cell proliferation and differentiation.[30] The pivotal role of FOXM1 in liver development and regeneration has been reported previously.[17] FOXM1 was also required for HCC development in a mouse hepatocarcinogenesis model[31] and acted as an oncogene in a transgenic mouse model.[32] It was recently shown that FOXM1 levels are elevated in various cancers including HCC.[32,33] A prognostic role for FOXM1 in HCC patients after liver transplantation was also reported[34]; this may be associated with the metastatic capacity of tumors regulated by FOXM1.[35] As FOXM1 and AFP are known to be activated during liver regeneration and hepatocarcinogenesis, serum AFP levels may be a surrogate marker for the expression status of FOXM1 and thus facilitate the prognostic stratification of HCCs by the EOB-AFP classification.

Among the molecular markers reported to be differentially expressed between dysplastic nodule and well-differentiated HCC, we found preferential overexpression of GS in EOB-AFP class A and GPC-3 in class C HCCs. Our data suggest that class A and class C HCCs may follow different processes of early hepatocarcinogenesis events that might be associated with the differential activation of HNF4α and FOXM1, and further studies are required to obtain molecular insights into these processes.

Our overall survival data in Cohort 2 indicated that EOB-AFP class A patients had 100% overall survival, whereas class C patients had 30% overall survival at 1,200 days after radical resection. This suggests that the micro-dissemination of tumor cells in EOB-AFP class C HCC patients has already occurred by the time they are diagnosed with early-stage disease. Indeed, 50% of all class C patients showed tumor recurrence, whereas 88-100% of class A patients showed no recurrence within 1 year of resection; this is consistent with a recent study evaluating the clinical features of hyperintense HCCs[36] and may be due to

the overexpression of FOXM1, which results in the activation of metastatic programs. Therefore, these patients might have survival benefits if they receive adjuvant therapies. As several adjuvant therapies might be beneficial for HCC patients after surgical resection,[37] integration of the EOB-AFP classification system into current staging practices may provide additional therapeutic options for early-stage HCC patients who will receive surgery.

A limitation of the present study is that we used three different cohorts to reveal the molecular portraits associated with clinical imaging and prognosis (i.e., the microarray cohort of 238 HCCs of various stages for the evaluation of molecular profiling; Cohort 1 for the validation of molecular profiling and EOB-MRI findings in various stages of HCC; and Cohort 2 for evaluating the utility of EOB-MRI and serum AFP in predicting the prognosis of early-stage HCCs), which made the molecular and prognostic analyses complex. Another limitation of this study was in the evaluation of prognostic utility because it uses small retrospective cohorts. Direct evaluation of the molecular profiles and prognostic values of hyperintense HCCs should be performed in a prospective study using a large-scale HCC cohort.

Taken together, the present study demonstrates for the first time that the combined approach of noninvasive Gd-EOB-DTPA-enhanced MRI and serum AFP levels can be used preoperatively to classify resectable HCCs into three subgroups with distinct prognoses. This classification is molecularly related to the stem/maturation status of HCCs regulated by HNF4α and FOXM1. The multicenter early-stage HCC cohort that received radical resection revealed that the EOB-AFP classification is clinically useful to determine the prognosis of early-stage HCC patients. On the basis of these observations, we propose that the EOB-AFP classification system be incorporated into current HCC staging practices, especially for the management of early-stage HCCs.

Acknowledgment: We thank Drs. Yutaka Aoyagi (Division of Gastroenterology and Hepatology, Niigata University Graduate School of Medical and Dental Sciences, Niigata, Japan), Hiroko Iijima (Division of Hepatobiliary and Pancreatic Disease, Department of Internal Medicine, Hyogo College of Medicine, Hyogo, Japan), and Michio Sata (Division of Gastroenterology, Department of Medicine, Kurume University School of Medicine, Kurume, Japan) for help with patient enrollment. We also thank Mss. Masayo Baba and Nami Nishiyama for excellent technical assistance.

References

1. Jemal A, Bray F, Center MM, Ferlay J, Ward E, Forman D. Global cancer statistics. CA Cancer J Clin 2011;61:69-90.
2. Sala M, Forner A, Varela M, Bruix J. Prognostic prediction in patients with hepatocellular carcinoma. Semin Liver Dis 2005;25:171-180.
3. Cairo S, Wang Y, de Reynies A, Duroure K, Dahan J, Redon MJ, et al. Stem cell-like micro-RNA signature driven by Myc in aggressive liver cancer. Proc Natl Acad Sci U S A 2010;107:20471-20476.
4. Lee JS, Heo J, Libbrecht L, Chu IS, Kaposi-Novak P, Calvisi DF, et al. A novel prognostic subtype of human hepatocellular carcinoma derived from hepatic progenitor cells. Nat Med 2006;12:410-416.
5. Marquardt JU, Raggi C, Andersen JB, Seo D, Avital I, Geller D, et al. Human hepatic cancer stem cells are characterized by common stemness traits and diverse oncogenic pathways. HEPATOLOGY 2011;54:1031-1042.
6. Yamashita T, Ji J, Budhu A, Forgues M, Yang W, Wang HY, et al. EpCAM-positive hepatocellular carcinoma cells are tumor-initiating cells with stem/progenitor cell features. Gastroenterology 2009;136:1012-1024.
7. Yamashita T, Wang XW. Cancer stem cells in the development of liver cancer. J Clin Invest 2013;123:1911-1918.
8. Reimer P, Schneider G, Schima W. Hepatobiliary contrast agents for contrast-enhanced MRI of the liver: properties, clinical development and applications. Eur Radiol 2004;14:559-578.
9. Kanki A, Tamada T, Higaki A, Noda Y, Tanimoto D, Sato T, et al. Hepatic parenchymal enhancement at Gd-EOB-DTPA-enhanced MR imaging: correlation with morphological grading of severity in cirrhosis and chronic hepatitis. Magn Reson Imaging 2012;30:356-360.
10. Kitao A, Matsui O, Yoneda N, Kozaka K, Shinmura R, Koda W, et al. The uptake transporter OATP8 expression decreases during multistep hepatocarcinogenesis: correlation with gadoxetic acid enhanced MR imaging. Eur Radiol 2011;21:2056-2066.
11. Kitao A, Zen Y, Matsui O, Gabata T, Kobayashi S, Koda W, et al. Hepatocellular carcinoma: signal intensity at gadoxetic acid-enhanced MR Imaging—correlation with molecular transporters and histopathologic features. Radiology 2010;256:817-826.
12. Yamashita T, Forgues M, Wang W, Kim JW, Ye Q, Jia H, et al. EpCAM and alpha-fetoprotein expression defines novel prognostic subtypes of hepatocellular carcinoma. Cancer Res 2008;68:1451-1461.
13. Yamashita T, Honda M, Nakamoto Y, Baba M, Nio K, Hara Y, et al. Discrete nature of EpCAM(+) and CD90(+) cancer stem cells in human hepatocellular carcinoma. HEPATOLOGY 2013;57:1484-1497.
14. Yamashita T, Honda M, Nio K, Nakamoto Y, Takamura H, Tani T, et al. Oncostatin m renders epithelial cell adhesion molecule-positive liver cancer stem cells sensitive to 5-Fluorouracil by inducing hepatocytic differentiation. Cancer Res 2010;70:4687-4697.
15. Lade AG, Monga SP. Beta-catenin signaling in hepatic development and progenitors: which way does the WNT blow? Dev Dyn 2011;240:486-500.
16. Trauner M, Halilbasic E. Nuclear receptors as new perspective for the management of liver diseases. Gastroenterology 2011;140:1120-1125 e1121-1112.
17. Wang X, Kiyokawa H, Dennewitz MB, Costa RH. The Forkhead Box m1b transcription factor is essential for hepatocyte DNA replication and mitosis during mouse liver regeneration. Proc Natl Acad Sci U S A 2002;99:16881-16886.
18. Hoshida Y, Villanueva A, Kobayashi M, Peix J, Chiang DY, Camargo A, et al. Gene expression in fixed tissues and outcome in hepatocellular carcinoma. N Engl J Med 2008;359:1995-2004.
19. Ji J, Shi J, Budhu A, Yu Z, Forgues M, Roessler S, et al. MicroRNA expression, survival, and response to interferon in liver cancer. N Engl J Med 2009;361:1437-1447.
20. Di Tommaso L, Destro A, Seok JY, Balladore E, Terracciano L, Sangiovanni A, et al. The application of markers (HSP70 GPC3 and GS) in liver biopsies is useful for detection of hepatocellular carcinoma. J Hepatol 2009;50:746-754.

21. Llovet JM, Chen Y, Wurmbach E, Roayaie S, Fiel MI, Schwartz M, et al. A molecular signature to discriminate dysplastic nodules from early hepatocellular carcinoma in HCV cirrhosis. Gastroenterology 2006;131:1758-1767.
22. Sherman M. Hepatocellular carcinoma: screening and staging. Clin Liver Dis 2011;15:323-334, vii-x.
23. Villanueva A, Hoshida Y, Toffanin S, Lachenmayer A, Alsinet C, Savic R, et al. New strategies in hepatocellular carcinoma: genomic prognostic markers. Clin Cancer Res 2010;16:4688-4694.
24. de Lope CR, Tremosini S, Forner A, Reig M, Bruix J. Management of HCC. J Hepatol 2012;56 Suppl:S75-87.
25. Crestani M, De Fabiani E, Caruso D, Mitro N, Gilardi F, Vigil Chacon AB, et al. LXR (liver X receptor) and HNF-4 (hepatocyte nuclear factor-4): key regulators in reverse cholesterol transport. Biochem Soc Trans 2004;32:92-96.
26. Bonzo JA, Ferry CH, Matsubara T, Kim JH, Gonzalez FJ. Suppression of hepatocyte proliferation by hepatocyte nuclear factor 4alpha in adult mice. J Biol Chem 2012;287:7345-7356.
27. Ning BF, Ding J, Yin C, Zhong W, Wu K, Zeng X, et al. Hepatocyte nuclear factor 4 alpha suppresses the development of hepatocellular carcinoma. Cancer Res 2010;70:7640-7651.
28. Yin C, Lin Y, Zhang X, Chen YX, Zeng X, Yue HY, et al. Differentiation therapy of hepatocellular carcinoma in mice with recombinant adenovirus carrying hepatocyte nuclear factor-4alpha gene. HEPATOLOGY 2008;48:1528-1539.
29. Hatziapostolou M, Polytarchou C, Aggelidou E, Drakaki A, Poultsides GA, Jaeger SA, et al. An HNF4alpha-miRNA inflammatory feedback circuit regulates hepatocellular oncogenesis. Cell 2011;147:1233-1247.
30. Koo CY, Muir KW, Lam EW. FOXM1: From cancer initiation to progression and treatment. Biochim Biophys Acta 2012;1819:28-37.
31. Kalinichenko VV, Major ML, Wang X, Petrovic V, Kuechle J, Yoder HM, et al. Foxm1b transcription factor is essential for development of hepatocellular carcinomas and is negatively regulated by the p19ARF tumor suppressor. Genes Dev 2004;18:830-850.
32. Kalin TV, Ustiyan V, Kalinichenko VV. Multiple faces of FoxM1 transcription factor: lessons from transgenic mouse models. Cell Cycle 2011;10:396-405.
33. Calvisi DF, Pinna F, Ladu S, Pellegrino R, Simile MM, Frau M, et al. Forkhead box M1B is a determinant of rat susceptibility to hepatocarcinogenesis and sustains ERK activity in human HCC. Gut 2009;58:679-687.
34. Sun H, Teng M, Liu J, Jin D, Wu J, Yan D, et al. FOXM1 expression predicts the prognosis in hepatocellular carcinoma patients after orthotopic liver transplantation combined with the Milan criteria. Cancer Lett 2011;306:214-222.
35. Raychaudhuri P, Park HJ. FoxM1: a master regulator of tumor metastasis. Cancer Res 2011;71:4329-4333.
36. Kitao A, Matsui O, Yoneda N, Kozaka K, Kobayashi S, Koda W, et al. Hypervascular hepatocellular carcinoma: correlation between biologic features and signal intensity on gadoxetic acid-enhanced MR images. Radiology 2012;265:780-789.
37. Zhong JF, Li H, Li LQ, You XM, Zhang Y, Zhao YN, et al. Adjuvant therapy options following curative treatment of hepatocellular carcinoma: a systematic review of randomized trials. Eur J Surg Oncol 2012;38:286-295.

Supporting Information

Additional Supporting Information may be found in the online version of this article at the publisher's website.

Hepatology Research

Hepatology Research 2014 doi: 10.1111/hepr.12436

Original Article

Blood neutrophil to lymphocyte ratio as a predictor in patients with advanced hepatocellular carcinoma treated with hepatic arterial infusion chemotherapy

Takeshi Terashima, Tatsuya Yamashita, Noriho Iida, Taro Yamashita, Hidetoshi Nakagawa, Kuniaki Arai, Kazuya Kitamura, Takashi Kagaya, Yoshio Sakai, Eishiro Mizukoshi, Masao Honda and Shuichi Kaneko

Department of Gastroenterology, Kanazawa University Hospital, Kanazawa, Ishikawa, Japan

Aim: Inflammation plays a critical role in cancer. The aim of the present study was to investigate the impact of neutrophil to lymphocyte ratio (NLR) on patients with advanced hepatocellular carcinoma (HCC) treated with hepatic arterial infusion chemotherapy (HAIC).

Methods: We retrospectively evaluated 266 patients with advanced HCC treated with HAIC between March 2003 and December 2012. NLR was calculated from the differential leukocyte count by dividing the absolute neutrophil count by the absolute lymphocyte count.

Results: The cut-off level of NLR was set as the median value of 2.87 among all patients in this study. The objective response rate in the patients with low NLR was 37.6%, which was significantly better than that of the patients with high NLR (21.1%; $P < 0.01$). Multivariate analysis revealed that low NLR remained associated with the response to HAIC ($P = 0.024$). Median progression-free survival and median overall survival in patients with high NLR were 3.2 and 8.0 months, respectively, which were significantly shorter than that of the patients with low NLR (5.6 and 20.7 months; $P < 0.01$ and $P < 0.01$, respectively). High NLR was an independent unfavorable prognostic factor in multivariate analysis. The patient outcome was stratified more clearly by NLR calculated after HAIC added to calculations before HAIC. Serum platelet-derived growth factor-BB level was positively correlated with NLR.

Conclusion: Results suggest that NLR is a useful predictor in patients with advanced HCC treated with HAIC. These findings may be useful in determining treatment strategies or in designing clinical chemotherapy trials in future.

Key words: hepatic arterial infusion chemotherapy, hepatocellular carcinoma, neutrophil lymphocyte ratio, predictive factor, prognostic factor

INTRODUCTION

HEPATOCELLULAR CARCINOMA (HCC) is the third leading cause of cancer death and remains a worldwide health concern because the incidence of HCC continues to increase globally.[1] A variety of new techniques of imaging modalities have enabled the detection of HCC at early stages, and advances of various therapeutic procedures have improved the curability of patients with HCC.[2] Despite those recent advances in diagnostic and therapeutic technologies, the prognosis of patients with HCC remains poor due to impaired liver function and frequent recurrence of HCC.[3]

Although sorafenib has been established as the standard of care for advanced HCC,[4] its efficacy and tolerability are limited.[5] As an alternative therapy to sorafenib, hepatic arterial infusion chemotherapy (HAIC) has been conducted in Asia, including Japan, and it has been reported as a promising treatment procedure.[6,7] However, application of HAIC and its predictive and prognostic markers have not been fully established.

Inflammation plays a critical role in the development and progression of various cancers.[8] Inflammation caused by extrinsic factors including a variety of infectious agents and environmental toxins, as well as intrinsic factors including active oncogenes, reactive

Correspondence: Dr Tatsuya Yamashita, Department of Gastroenterology, Kanazawa University Hospital, 13-1 Takara-machi, Kanazawa, Ishikawa 920-8641, Japan. Email: ytatsuya@m-kanazawa.jp

Conflicts of interest: None to declare.

Received 1 September 2014; revision 3 October 2014; accepted 11 October 2014.

oxygen species and necrosis existing in the cancer tissues, promote various processes of cancer initiation and progression, such as mutation, proliferation, immortalization, invasiveness, angiogenesis, epithelial–mesenchymal transition and immunosuppression.[9] Additionally, the release of inflammation-related substances is closely related to symptoms such as loss of bodyweight, fatigue and appetite loss among cancer patients. Therefore, inflammation-induced cancer progression and cachectic patient status affect quality of life and patient outcomes.[10] The inflammation-related markers such as absolute white blood cell count, C-reactive protein (CRP), neutrophil to lymphocyte ratio (NLR), platelet to lymphocyte ratio and cytokines have been suggested to be associated with outcomes of patients with various malignancies[11] including at an early or intermediate disease stage of HCC.[12–16] However, whether these markers can serve as biomarkers of treatment efficacies and patient outcome in more advanced stages of HCC remains unclear.

The objectives of the present study were to investigate the correlation between NLR and patient characteristics in advanced HCC patients. We also analyzed the impact of NLR on the treatment efficacies as well as the outcome of patients with advanced HCC treated with HAIC. Moreover, to assess inflammatory molecules associated with NLR, serum level of cytokines and growth factors were measured. This approach provides useful information in determining treatment strategies for patients with advanced HCC.

METHODS

Patients

THE SUBJECTS IN this study were patients treated with HAIC at the Kanazawa University Hospital between March 2003 and December 2012 for advanced HCC with vascular invasion and/or intrahepatic multiple lesions considered unsuitable for surgical resection, locoregional therapy and transarterial chemoembolization. All patients underwent dynamic computed tomography (CT) or dynamic magnetic resonance imaging (MRI) to diagnose HCC and assess the extent of cancer. Additionally, HCC was diagnosed according to the guidelines of the American Association for the Study of Liver Disease.[17] Patients with extrahepatic lesions were also considered eligible for HAIC if their extrahepatic lesions were mild; intrahepatic lesions were considered to be prognostic factors. Other inclusion criteria were Eastern Cooperative Oncology Group performance status (ECOG PS) of 2 or less, appropriate major organ functions, including bone marrow, kidney, cardiac functions and hepatic function (Child–Pugh A or B), and no clinical symptoms or signs of sepsis.

HAIC

The technique for implantation of the reservoir system has been thoroughly described elsewhere.[18] Catheters were induced through the right femoral artery and angiography from the celiac artery was first performed to localize the HCC and evaluate the intrahepatic and extrahepatic vascularization. Then, we inserted a catheter with a side opening into the gastroduodenal artery, positioning the side opening in the common hepatic artery by an image-guided procedure. The gastroduodenal artery, right gastric artery and other arteries that were suspected to nourish the gastroduodenal region were embolized as much as possible to prevent the gastrointestinal mucositis. The other end of the catheter was connected to the injection port subcutaneously implanted in the right lower abdomen. Finally, we confirmed blood flow redistribution.

Hepatic arterial infusion chemotherapy was conducted approximately 5 days after the reservoir was implanted. The treatment protocol was as follows: all patients received 5-fluorouracil (FU) (330 mg/m^2 per day) administrated continuously for 24 h from day 1 to day 5 and day 8 to day 12, and either interferon (IFN)-α-2b or pegylated (PEG) IFN-α-2b used at the treating physician's discretion. PEG IFN-α-2b (1.0 μg/kg) was administrated s.c. on days 1, 8, 15 and 22, and IFN-α-2b (3×10^6 U) was administrated i.m. thrice weekly. Some patients underwent cisplatin administration (20 mg/m^2 per day) into the hepatic artery for 10 min prior to 5-FU. A treatment cycle consisted of 28 days of drug administration, followed by a 14-day rest period. The treatment was repeated until tumor progression or unacceptable toxicity was observed, or until the patient refused the treatment. The treatment protocol was approved by the ethics Committee of Kanazawa University, and informed consent for participation in the study was obtained from each subject and conformed to the guidelines of the 1975 Declaration of Helsinki.

Data collection

We reviewed the medical records of the patients, and collected demographic, clinical and laboratory data, including patient age, sex, ECOG PS, history of viral infection, hepatic reserve (Child–Pugh score), imaging data (vascular invasion and extrahepatic lesion) and tumor marker analyses. We collected laboratory data on complete blood count and CRP. The NLR was calculated

from the differential leukocyte count by dividing the absolute neutrophil count by the absolute lymphocyte count. We used the laboratory data obtained within 7 days prior to day 1 of treatment in this study. We also collected NLR values at 4 weeks after the treatment began to evaluate the impact of the NLR trend on patient outcomes. Cytokine and chemokine profiling was obtained as described below:[19] after venous blood was centrifuged at 1580 *g* for 10 min at 4°C, serum fractions were obtained and stored at −20°C until used. Serum levels of various cytokines and chemokines were measured using the Bio-Plex Protein Array System (Bio-Rad, Richmond, CA, USA) according to the manufacturer's protocol. Briefly, frozen serum samples were thawed at room temperature, diluted 1:4 in sample diluents, and 50 μL aliquots of diluted sample were added in duplicate to the wells of 96-well microtiter plates containing the coated beads for a validated panel of human cytokines and chemokines according to the manufacturer's instructions. The following 20 cytokines and chemokines were targeted: epidermal growth factor (EGF), basic fibroblast growth factor, hepatocyte growth factor, IFN-γ, interleukin (IL)-2, IL-4, tumor necrosis factor-α (TNF-α), IL-6, IL-8, IL-10, IL-5, IFN γ-induced protein (IP)-10, monokine induced by IFN-γ (MIG), platelet-derived growth factor (PDGF)-BB, transforming growth factor (TGF)-β, TGF-α, vascular endothelial growth factor (VEGF), stem cell factor, IL-12 and stromal cell-derived factor 1. Nine standards (range, 0.5–32 000 pg/mL) were used to generate calibration curves for each cytokine. Data acquisition and analysis were performed using Bio-Plex Manager software version 4.1.1 (Bio-Rad).

Evaluation of antitumor effect

The efficacy of HAIC was assessed every 4–6 weeks by dynamic CT or dynamic MRI during the treatment period. The response to chemotherapy was assessed by treating physicians according to the Response Evaluation Criteria in Solid Tumors version 1.1.[20] An objective response rate was defined as the sum of complete response rate and partial response rate.

Statistical analysis

We compared patient backgrounds according to NLR and patient demographics using the χ^2-test for categorical variables when appropriate. Student's *t*-test and Mann–Whitney *U*-test were used for continuous variables. We set the cut-off level of continuous variables as the median value among all patients in this study. We divided the patients into two groups according to NLR before and after treatment, respectively, and compared the response to HAIC and patient outcome between groups. The χ^2-test was also used to evaluate the relation between NLR and the response to HAIC in univariate analysis. Logistic regression analysis was used for multivariate analysis. Progression-free survival (PFS) was calculated from the first day of HAIC until the date of radiological progression, death or the last day of the follow-up period. Overall survival (OS) was calculated from the first day of HAIC until the date of death or the last day of the follow-up period. To compare PFS and OS between groups, the cumulative survival proportions were calculated using the Kaplan–Meier method, and any differences were evaluated using the log–rank test. Only variables that achieved statistical significance in the univariate analysis were subsequently evaluated in the multivariate analysis using Cox's proportional hazards regression model. Linear regression was used to explore the relationship between cytokine or chemokine profiling and NLR. A *P*-value of less than 0.05 was considered statistically significant. All statistical analyses were performed using the SPSS statistical software program package (SPSS, Chicago, IL, USA).

RESULTS

Patients characteristics stratified by NLR

WE RETROSPECTIVELY LISTED 267 consecutive patients who met the above-described criteria and reviewed their medical records. The information regarding the differential leukocyte count could not be obtained in one patient, and then the remaining 266 patients were analyzed. One hundred and thirty-three (50.0%) of 266 patients had NLR higher than 2.87, the median value among all patients before treatment. Patient demographic characteristics are summarized in Table 1. Patients with high NLR had a significantly worse performance status than those with low NLR ($P = 0.020$). With regard to tumor status, vascular invasion and extrahepatic dissemination were observed more often in the patients with high NLR (57.1% and 27.8%, respectively) than in those with low NLR (39.8% and 18.0%, respectively), and des-γ-carboxyprothrombin (DCP) was higher in the group with high NLR (median, 1286 mAU/mL) than in the one with low NLR (median, 214 mAU/mL). Sorafenib was administrated as prior treatment before HAIC in 25 patients (9.4%) and as subsequent therapy after HAIC in 26 patients (9.8%). The proportion of the patients receiving sorafenib before HAIC was similar between the two groups, whereas the proportion of the patients

Table 1 Clinical characteristic of the patients according to NLR

	All ($n = 266$)	High NLR ($n = 133$)	Low NLR ($n = 133$)	P
Age, years				<0.01*
Mean ± SD	66.3 ± 9.1	64.7 ± 9.9	68.0 ± 7.8	
Sex, *n* (%)				0.30**
Male	209 (78.6)	108 (81.2)	101 (75.9)	
ECOG PS, *n* (%)				0.020**
0	220 (82.7)	103 (77.4)	117 (88.0)	
1	41 (15.4)	25 (18.8)	16 (12.0)	
2	5 (1.9)	5 (3.8)	0	
Sorafenib before HAIC				0.83**
Present	25 (9.4)	12 (9.0)	13 (9.8)	
Sorafenib after HAIC				0.013**
Present	26 (9.8)	19 (14.3)	7 (5.3)	
HBs antigen, *n* (%)				0.27**
Positive	70 (26.3)	39 (29.3)	31 (23.3)	
HCV antibody, *n* (%)				<0.01**
Positive	146 (54.9)	57 (42.9)	89 (66.9)	
Child-Pugh score, *n* (%)				0.34**
5–6	134 (50.4)	61 (45.9)	73 (54.9)	
7	55 (20.7)	30 (22.6)	25 (18.8)	
8–9	77 (28.9)	42 (31.6)	35 (26.3)	
Vascular invasion, *n* (%)				<0.01**
Positive	129 (48.5)	76 (57.1)	53 (39.8)	
Extrahepatic lesion, *n* (%)				0.058**
Positive	61 (22.9)	37 (27.8)	24 (18.0)	
CRP, mg/dL				<0.01*
Mean ± SD	1,9 ± 3.0	2.8 ± 3.8	0.9 ± 1.2	
AFP, ng/mL				0.41***
Median, range	241.5, <10–1 637 200	312.5, <10–745 900	119.5, <10–1 637 200	
DCP, mAU/mL				<0.01***
Median, range	567, <10–1 208 000	1 286, <10–1 208 000	214, <10–326 300	

*Student's *t*-test, **χ^2-test, ***Mann–Whitney *U*-test.
AFP, α-fetoprotein; CRP, C-reactive protein; DCP, des-γ-carboxyprothrombin; ECOG PS, Eastern Cooperative Oncology Group performance status; HBs antigen, hepatitis B surface antigen; HCV antibody, hepatitis C virus antibody; NLR, neutrophil to lymphocyte ratio; SD, standard deviation.

receiving sorafenib after HAIC was higher in the group with high NLR (14.3%) than in the one with low NLR (5.3%) ($P = 0.013$).

Treatment

The data collection cut-off was 20 April, 2014. The median follow-up period was 11.4 months (range, 0.3–127.6). At the time of the analysis, 212 patients (79.7%) had died. A total of 715 courses were administrated to 266 patients, with a median number of two (range, 0–13). All but 18 patients including 12 patients (9.0%) in the high NLR group and six (4.5%) in the low NLR group completed at least one course of HAIC.

Of the 266 patients, IFN-α-2b and PEG IFN-α-2b was used in 131 patients (49.2%) and 135 patients (50.8%), respectively. The response to HAIC and the patient outcomes were similar between the different IFN groups. Cisplatin was administrated in 186 patients (69.9%). Although response to HAIC had a tendency to be better in patients in the cisplatin group than those of the patients without cisplatin, there was no significant differences of the treatment efficacies.

Response to HAIC and PFS stratified by pretreatment NLR

Of the 266 patients, 15 patients could not receive radiological assessment because of worsened general condition, hepatic failure or loss to follow up, and the remaining 251 were assessable for response to treatment. The tumor responses to HAIC are shown in